SieveNet

Estimating the Particle Size Distribution of Kernel Fragments in Whole Plant Corn Silage

Rasmussen, Christoffer Bøgelund; Kirk, Kristian; Moeslund, Thomas B.

Published in:
Proceedings of the 17th International Joint Conference on Computer Vision, Imaging and Computer Graphics Theory and Applications - Volume 5: VISAPP

DOI (link to publication from Publisher):
10.5220/0010821200003124

Publication date:
2022

Document Version
Publisher's PDF, also known as Version of record

SieveNet: Estimating the Particle Size Distribution of Kernel Fragments in Whole Plant Corn Silage

Christoffer Bøgelund Rasmussen[1][a], Kristian Kirk[2] and Thomas B. Moeslund[1][b]
[1]*Visual Analysis and Perception Lab, Aalborg University, Rendsburggade 14, 9000 Aalborg, Denmark*
[2]*CLAAS E-Systems, Møllevej 11, 2990 Nivå, Denmark*

Keywords: Object Recognition, Convolutional Neural Networks, Region Proposal Network, Kernel Fragmentation, Whole Plant Corn Silage.

Abstract: In this paper we present a method for efficiently measuring the particle size distribution of whole plant corn silage with a sieving-based network. Our network, SieveNet, learns to predict the size class of predefined sieves for kernel fragments through a novel sieve-based anchor matching algorithm during training. SieveNet improves inference timings by 40% compared to previous approaches that are based on two-stage recognition networks. Additionally, an estimated Corn Silage Processing score from the network predictions show strong correlations of up to 0.93 r^2 against physically sieved samples, improving correlation results by a number of percentage points compared to previous approaches.

1 INTRODUCTION

Efficient evaluation of Whole Plant Corn Silage (WPCS) is an important step to determine if the plant is correctly harvested with a forage harvester. One key parameter is the appropriate processing of kernels into smaller fragments. The fragmentation of the corn kernels allows for more efficient and higher quality fodder for dairy cows (Mertens, 2005) and is achieved by altering the processing gap in the kernel processor in the harvester. By evaluating the kernel processing a farmer is able to react in the field to suboptimal settings or variation across their field. An efficient evaluation can be beneficial as modern forage harvester are able to harvest multiple tonnes per hour (Marsh, 2013). However, current industry standards are based upon determining the particle size distribution (PSD) of a WPCS sample with manual sieving techniques which require potentially errorsome manual preparation steps. Examples include the Corn Silage Processing Score (CSPS) that measures the percentage of kernel fragments passing a 4.75 mm sieve (Mertens, 2005) or the Penn State Particle Separator that determines the distribution over three to four differently sized sieves (Heinrichs and Coleen, 2016).

Compared to previous similar works on evaluating WPCS our approach is considerably simpler. Previous works have trained two-stage object recognition networks in the form of bounding-box detectors or instance segmentation networks for fine-grain localisation (Rasmussen and Moeslund, 2019) (Rasmussen et al., 2021). Then for a set of predictions over a number of images the length of the major axis was compared against the CSPS quality metric. Instead in this work we propose to discard the second stage in the two-stage networks and only adopt an altered Region Proposal Network (RPN). We introduce the network SieveNet that aims to mimic the sieving process that allow for measurements such as CSPS. The network uses a novel anchor matching algorithm during training that allows the network to learn how to classify which sieve size a kernel fragment instance would lie in during sieving. Traditionally, anchors in the RPN are used as dense bounding-box priors of varying sizes computed over the entire feature map producing object proposals with class-agnostic objectness scores and box refinement deltas. This scheme is altered in SieveNet by defining anchors based on a number of sieving sizes and during training positive anchors are matched using a set of criterion based on sieving. The criterion are:

1. A matched bounding-box anchor should have a diameter smaller than that of the ground truth diameter.

[a] https://orcid.org/0000-0002-8786-0737
[b] https://orcid.org/0000-0001-7584-5209

Rasmussen, C., Kirk, K. and Moeslund, T.
SieveNet: Estimating the Particle Size Distribution of Kernel Fragments in Whole Plant Corn Silage.
DOI: 10.5220/0010821200003124
In *Proceedings of the 17th International Joint Conference on Computer Vision, Imaging and Computer Graphics Theory and Applications (VISIGRAPP 2022) - Volume 5: VISAPP*, pages 117-124
ISBN: 978-989-758-555-5; ISSN: 2184-4321

2. The matched bounding-box anchor should be the that which has the smallest difference between the anchor diameter and ground truth diameter.
3. Only a single anchor sieve size can be matched to a ground truth instance.

We adopt the same dataset as the two-stage recognition networks (Rasmussen and Moeslund, 2019) (Rasmussen et al., 2021) which exhibits a high amount of clutter amongst kernel fragments. An example image from the dataset can be seen in Figure 1 visualising annotated kernel fragments by a white outline.

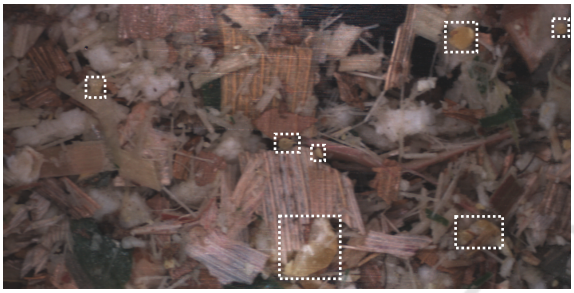

Figure 1: Example of WPCS with annotations of kernel fragments.

The above sieving criteria implemented on the dataset are visualised for a single instance in Figure 2 highlighting the difference between traditional RPN matching (Ren et al., 2015) and our novel sieve-based matcher. In both examples a ground truth kernel fragment bounding-box is highlighted by a dashed white outline. In Figure 2b, during training a positive label is given to the anchors with an Intersection-over-Union (IoU) greater than 0.7, which in this case are marked in green. However, in our approach in Figure 2c two positive examples are now marked as negatives are their diameter is greater than that of the ground truth. Additionally, only a single positive match is found which is the first anchor with a smaller diameter. The only requirement we introduce on intersection is that it must be greater than 0, therefore, in theory as long as the three criteria above are met the intersection between anchor and ground truth can be small.

In comparison to an RPN the SieveNet is simplified in regards to network training as bounding-box regression is not required as we are only interested in the classification of instances into a fixed sieve class. We show in this work that it is possible to train our SieveNet to accurately and efficiently estimate the sieving of WPCS. Finally, compared to previous works we show competitive results in comparison to physically sieved samples at a considerable reduction in inference time.

(a) Reference bounding-box annotation.

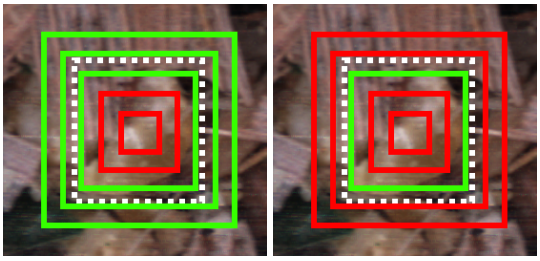

(b) Traditional RPN-based anchor matching. (c) SieveNet-based anchor matching.

Figure 2: Overview of matching strategies between RPN IoU (a) and SieveNet (b).

Our contribution in this work is:

- A novel sieve-based matching algorithm.
- Show that a Region Proposal Network is able to learn to classify a specific bounding-box anchor.
- Improve the speed of kernel fragmentation analysis in WPCS compared to previous methods without compromising CSPS estimation against real-world samples.

2 RELATED WORK

Measurement of WPCS through computer vision is limited. Overall there have been two general methodologies; methods that first separate a sample of WPCS such that kernel fragments can easier be localised and methods that analyse images of samples without the need for separation. Within the separation-based approaches, the contours of kernel fragments spread out on a black background were found using maximally stable external regions from which the maximum inscribed circle was compared to determine CSPS (Drewry et al., 2019). However, the manual separation steps can be cumbersome to conduct especially for a farmer in the field. Additionally, laboratory equipment is required which can make the process time-consuming and does not allow the farmer to re-

act to their field conditions during the harvest. To address this a number of works have estimated CSPS on non-separated samples of WPCS. Firstly, two-stage object recognition networks in the form of Multi-task Network Cascades and Region-based Fully Convolutional Networks were trained from which CSPS was estimated from instance masks or bounding-boxes and compared against CSPS estimated from annotations (Rasmussen and Moeslund, 2019). A two-stage Faster R-CNN network was optimised by altering the anchor priors in the RPN by sampling the shapes of training bounding-boxes with k-means clustering (Rasmussen et al., 2021). This work also compared model estimated CSPS from the bounding-boxes against a number of physically sieved samples showing a strong correlation over a number of different machine settings. While the works on non-separated samples show good correlation results the networks exhibit a higher range of complexity making them not suitable for an embedded system where processing power is limited. Additionally, the two-stage pipeline of region proposals followed by box refinement may be superfluous as the final predictions end up being compared against a single CSPS threshold.

In other domains a number of works attempt to measure the size distribution of objects. These include determining the PSD of overlapping iron ore using hand-crafted shape and size features (Andersson et al., 2007). A U-Net based semantic segmentation network has also been used to localise iron ore pellets (Duan et al., 2020). The grain size of beach pebbles were estimated using a Mask R-CNN showing positive correlation when mapping the size results against measured samples (Soloy et al., 2020). A novel multi-task network architecture, HistoNet, has been used to predict a count map and a histogram without the need for fine-grain localisation of objects in cluttered scenes (Sharma et al., 2020). This work aims to move away from the complex pipeline found in object recognition networks and show impressive results compared to a Mask R-CNN. A significant amount of the training data is simulated which is possible due to the lower amount of variation in colour and texture in the images.

Other examples exist in literature of the RPN being utilised to localise objects without using the second half of the two-stage pipeline. Firstly, the generalisation of the RPN has been analysed on a number of benchmark datasets for multispectral person detection showing that the network could produce good quality predictions (Fritz et al., 2019). An RPN with a custom backbone architecture has been used to localise organs in 3D images from CT scans (Xu et al., 2019). The authors also included multi-class scores and together with box refinement and fusion of 3D feature data provided accurate results.

3 METHODOLOGY

SieveNet is built upon the RPN introduced in Faster R-CNN (Ren et al., 2015) with a ResNet50 (He et al., 2016) backbone within the Pytorch Detectron2 (Wu et al., 2019) framework. The aim of SieveNet is to efficiently determine the PSD within an RGB image given user-defined priors giving sieve sizes. Additionally, the network follows the supervised-learning mantra and therefore requires annotated instances of relevant objects in bounding-box format. The novel matching algorithm between anchors and ground truth boxes moves away from a purely Intersection-over-Union (IoU) criteria but rather matches based upon how an instance would be sieved. For example, a kernel fragment with a diameter of x would pass sieves which have a diameter greater than x but not those which are smaller. Therefore, our matching algorithm finds for each ground truth instance the anchor diameter that matches the sieving criterion defined earlier.

3.1 Dataset

We adopt the dataset for training SieveNet first presented in the works for performing object recognition for kernel fragmentation with two-stage networks (Rasmussen and Moeslund, 2019). The dataset contains a total of 2438 images containing 11601 annotated kernel fragments split over a training, validation and test sets.

3.2 Anchor Matching

The matching of anchors as positive or negative samples during training in the traditional RPN is based upon an IoU approach between the anchor and ground truth boxes at each sliding window location. If a given anchor has an IoU above a certain threshold with a ground truth box the anchor is labelled as a potential positive sample, anchors with an IoU below another threshold are labelled as negatives and finally the anchor boxes with an IoU between the two threshold are given an ignore label. Typical threshold values defined in the original introduction of the RPN in Faster R-CNN (Ren et al., 2015) are 0.7 for positives and 0.3 for negatives, however, these can be altered to a given use-case. Finally, a distribution of positive and negative boxes are sampled for each image

during training with the network learning the class-agnostic probability between object and background. As mentioned, this matching strategy is not sufficient for efficiently estimating PSD given a sieving criteria as positive matches can include boxes where either the anchor or ground truth has the larger diameter. Additionally, depending on the chosen anchor prior multiple anchors can be labelled as positives as long as each IoU is greater than the chosen threshold.

Our approach to anchor matching is first to define anchor shapes that match a potential sieving system which could be used to estimate CSPS. A total of five anchor sieves are chosen ranging from 1 mm to 9 mm in increments of 2 mm. Due to the constant distance between camera and samples when capturing images in the dataset this equates to pixel ranges between 20 and 180 at increments of 20. An overview of the sieve matching is covered in Algorithm 1. First, for a set of ground truth boxes the IoU is calculated with the anchors at each position in the feature map. Next, for all ground truth boxes and anchor boxes the diameters of each box is determined, for ground truth boxes the diameter is taken is the larger of the two axes. Then for each coordinate in the feature map with an IoU greater than zero the five anchor diameters are compared to the given ground truth diameter and the anchor diameters that are smaller are given a positive label. Anchor diameters that are greater represent sieves where the instance would pass are given a negative label. Once completed for all ground truth boxes, at each coordinate with multiple positives the positive anchors that do not have the smallest diameter and are set to negatives. At this point at each coordinate with an initial IoU greater than zero the correct sieve-based anchor is now matched. Finally, Non-Maximum Suppression (NMS) is applied for positive anchor labels at a threshold of 0.9 where anchors that overlap greatest with the ground truth are prioritised for training samples.

The number of positive samples is significantly different when adopting the matching approach compared to the IoU matching. In our networks we do not take into account an IoU threshold and allow matches do be set as long as the IoU is greater than zero. This approach mimics sieving better as a correctly sieved object may be considerably larger than the sieve/anchor resulting in a poor IoU. An alternative to our matching method is to adopt the Intersection-over-Area (IoA) metric in the RPN matching step. In IoA the overlap is defined as the area of the intersection over the area of the anchor box. A potentially more relevant metric is our sieve matching only uses cases where the anchor is the smaller of the two boxes. Table 1 shows the difference in the number of positive samples for the images in the training set before applying NMS to find the highest quality matches. A considerably larger amount of positive examples exist when using the IoA metric compared to IoU in the RPN matching equating to on average around 88 samples compared to 10. This is likely due to smaller anchors encapsulated by a ground truth scoring 1.0 instead of a potentially much lower score with IoU. Finally, our approach finds 2.75× more positives than the IoU approach despite only allowing a single anchor match at each location, however, we do match positives independent of any intersection based metric.

Algorithm 1: Anchor matching algorithm for SieveNet.

```
function SIEVEMATCHER(gtboxes, anchors)
    Calculate IoU(gtboxes, anchors)
    Calculate diameters of GT boxes
    Calculate diameters of anchor boxes
    for each coordinate with IoU > 0 do
        if Anchor diameter < GT diameter then
            anchor label = 0
        else
            anchor label = 1
        end if
    end for
    for Coordinates with multiple label == 1 do
        Find smallest anchor diameter label == 1
        Anchor labels where not smallest = 0
    end for
    NMS at threshold 0.9 for positive anchors
     return Anchor labels
end function
```

Table 1: Number of positive samples for the different matching methods for all images in the training set.

Matcher	Positive Samples
RPN IoU	14026
RPN IoA	122966
SieveNet	38652

Finally, we perform our sieve matching at a stride of 1 in the feature map. Other options exist, however, care should be taken dependent on the chosen backbone architecture. In our case, with ResNet50, the backbone down samples the input image throughout the network by a number of pooling and striding operations resulting in a feature map four times smaller. Therefore, when applying anchor matching at a stride of 1 this equates to a stride of 8 pixels in the input. For SieveNet with ResNet50 this difference is negligible but with a different architecture or changing the stride in the feature map may result in lower effectiveness in the matching step.

During inference the anchor matching step is naturally not included. Instead, the SieveNet uses a sliding window at the stride of 1 over the feature map and predict the probability of each anchor matching with a kernel fragment. Then predictions are thresholded based upon a confidence score and NMS thresholds predictions at an IoU of 0.05 leaving the final sieved predictions.

3.3 Model Training

The SieveNet with the anchor matching strategy presented in the previous section are trained for a total of 25000 iterations using stochastic gradient descent with a base learning rate of 0.025 and a batch size of four. Images are rescaled such that the shortest axis is 600 pixels and horizontal flipping augmentation is applied to double the amount of images. The training and inference of the models used for the results presented in the next section are done on an NVIDIA Titan XP GPU. During evaluation of the networks we take the given network iteration with the lowest validation loss.

4 RESULTS

In this section we present results from SieveNet models. This includes studies comparing both within model SieveNet variants are against an RPN with the classic matching algorithm. To make the results comparable between SieveNet and the RPNs we also remove bounding-box refinement from the RPNs. We present correlation results for models based upon the dataset of physically sieved samples for CSPS from two harvest weeks presented in (Rasmussen et al., 2021) and compare against the Faster R-CNN models from the same work. The data for the samples includes image sets and CSPS scores for a number of harvest runs containing machine setting altering the kernel fragmentation. For an image set we run our models over all images and estimate the CSPS by determining the percentage of predictions that pass the 5 mm anchor. When evaluating the models we present results with the Pearson Correlation Coefficient (PCC), r^2 coefficient of determination and the Root Mean Square Error (RMSE) comparing estimated model CSPS and physically sieved CSPS.

4.1 Matching Strategy

In Figures 3a and 3b example predictions from the same image are shown for RPN trained with the IoU and IoA respectively, where in Figures 3c predictions for SieveNet are shown. The example predictions in Figure 3b show the limitations of using an IoA based approach with RPN original matching approach. Here, any anchors that are within the bounds of a ground truth measure as 1.0 resulting in many small anchors being matched per ground truth. Additionally, as no bounding-box refinement is learnt NMS cannot be used to discard multiple anchors covering the same instance. Both RPN with the IoU metric and SieveNet show visually promising results appearing to match anchor boxes well with kernel fragment instances.

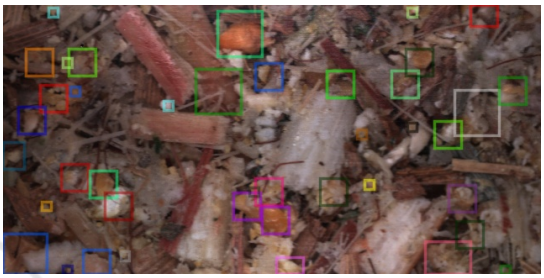

(a) RPN IoU.

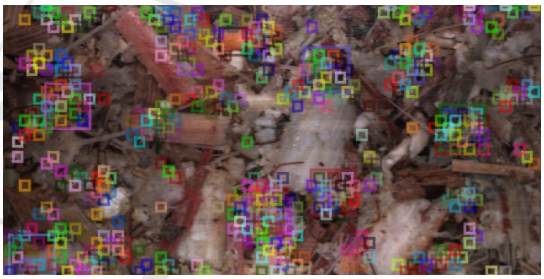

(b) RPN IoA.

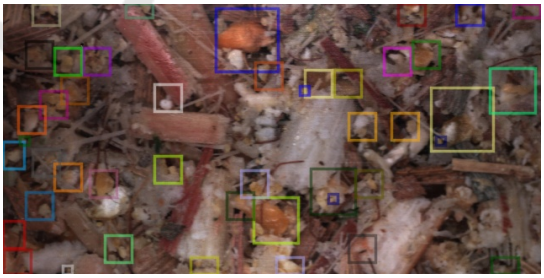

(c) SieveNet

Figure 3: Example predictions from models trained on different matching strategies.

Table 2 shows correlation results at three different confidence thresholds for each of the matching methods. Each approach show strong correlation scores, the RPN methods adopting an IoU threshold shows similar results in terms of PCC and r^2 compared to previous Faster R-CNN approaches. However, correlation scores decrease when adopting IoA especially

Table 2: Correlation results for previous works with Faster R-CNN (FRCNN) and our three networks with different matching strategies for two separate harvest weeks.

	CW40			CW43		
Model	PCC	r^2	RMSE	PCC	r^2	RMSE
FRCNN Baseline (Rasmussen et al., 2021)	0.68	0.46	8.12	0.64	0.41	17.09
FRCNN 2a (conf: 0.5) (Rasmussen et al., 2021)	0.84	0.70	**5.39**	0.63	0.40	8.89
FRCNN 2a (conf 0.25) (Rasmussen et al., 2021)	0.90	0.80	8.90	0.66	0.44	7.64
FRCNN 2a (conf 0.05) (Rasmussen et al., 2021)	0.91	0.84	18.87	0.77	0.59	16.23
RPN IoU (conf 0.5)	0.88	0.78	18.93	0.69	0.49	14.70
RPN IoU (conf 0.25)	0.89	0.79	19.90	0.74	0.54	16.09
RPN IoU (conf 0.05)	0.89	0.79	21.49	0.75	0.56	17.78
RPN IoA (conf 0.5)	0.82	0.67	31.38	0.47	0.22	27.80
RPN IoA (conf 0.25)	0.81	0.65	31.35	0.41	0.17	27.81
RPN IoA (conf 0.05)	0.80	0.64	31.34	0.38	0.15	27.73
SieveNet (conf 0.5)	**0.96**	**0.93**	10.12	0.74	0.54	**7.50**
SieveNet (conf 0.25)	0.95	0.90	14.27	**0.81**	**0.66**	10.70
SieveNet (conf 0.05)	0.85	0.73	31.11	0.44	0.19	27.42

for the CW43 dataset. SieveNet improves the results for both harvest weeks increasing both PCC and r^2 by a number of percentage points. For each of the approaches it can also be seen that the confidence threshold has an effect on CSPS correlation. For SieveNet there appears to be a good trade-off at confidence 0.25 show strong results for both weeks.

When evaluating the correlation results for both harvest weeks together SieveNet does show a slight decrease compared to Faster R-CNN as shown in Table 3.

Table 3: Correlation results for previous works with Faster R-CNN (FRCNN) and our three networks for a combined correlation over both harvest weeks.

	CW40+ CW43		
Model	PCC	r^2	RMSE
FRCNN Baseline (Rasmussen et al., 2021)	0.53	0.28	14.2
FRCNN 2a (conf: 0.5) (Rasmussen et al., 2021)	0.64	0.40	**7.69**
FRCNN 2a (conf: 0.25) (Rasmussen et al., 2021)	0.71	0.51	8.17
FRCNN 2a (conf: 0.05) (Rasmussen et al., 2021)	**0.81**	**0.66**	17.34
RPN IoU (conf: 0.5)	0.70	0.49	16.50
RPN IoU (conf: 0.25)	0.75	0.56	17.71
RPN IoU (conf: 0.05)	0.76	0.58	19.35
RPN IoA (conf: 0.5)	0.43	0.19	29.29
RPN IoA (conf: 0.25)	0.43	0.18	29.28
RPN IoA (conf: 0.05)	0.30	0.09	29.23
SieveNet (conf: 0.5)	0.75	0.56	8.65
SieveNet (conf: 0.25)	0.80	0.64	12.27
SieveNet (conf: 0.05)	0.48	0.23	27.23

Figure 4 shows a scatter plot of physical CSPS measured for each sample compared to estimated model CSPS for the image sets from CW40 and CW43 which are also shown in Table 2. We see the positive correlation for all three approaches, especially strong at the values from SieveNet with well aligned points.

Finally, we see that in Table 4 that SieveNet improves the inference time by almost 40% compared to Faster R-CNN when evaluating an inference image on an NVIDIA Titan XP GPU.

Table 4: Timings for networks on an NVIDIA Titan XP GPU.

Model	Inference Time (ms)
FRCNN 2a (Rasmussen et al., 2021)	51.1
SieveNet	**34.1**

4.2 Number of Anchors

For WPCS estimating the physical characteristics of the harvested crop our aim can be to predict the CSPS of a sample. For CSPS only the single sieve of 4.75 mm is required but in practice is typically done with multiple different sizes. In this section we evaluate training a SieveNet with two anchors, one for a 4.75 mm sieve and a smaller anchor at 1 mm capturing particles that pass the CSPS threshold anchor.

Figure 5 shows an example prediction from SieveNet with either two or five anchors. At the former in Figure 5a the restriction of not adopting box refinement allowing for further NMS is clear. Smaller fragments passing the larger 4.75 mm sieve that are more than double the size of the smallest anchor have

Table 5: Correlation for the two harvest weeks with previous results and additionally SieveNet with two anchors.

	CW40			CW43		
Model	PCC	r^2	RMSE	PCC	r^2	RMSE
FRCNN Baseline (Rasmussen et al., 2021)	0.68	0.46	8.12	0.64	0.41	17.09
FRCNN 2a (conf: 0.5) (Rasmussen et al., 2021)	0.84	0.70	**5.39**	0.63	0.40	8.89
FRCNN 2a (conf 0.25) (Rasmussen et al., 2021)	0.90	0.80	8.90	0.66	0.44	7.64
FRCNN 2a (conf 0.05) (Rasmussen et al., 2021)	0.91	0.84	18.87	0.77	0.59	16.23
RPN IoU (conf 0.25)	0.89	0.79	19.90	0.74	0.54	16.09
RPN IoA (conf 0.25)	0.81	0.65	31.35	0.41	0.17	27.81
SieveNet (conf 0.25)	**0.95**	**0.90**	14.27	**0.81**	**0.66**	10.70
SieveNet two anchors (conf 0.25)	0.38	0.15	29.42	-0.17	0.3	23.32

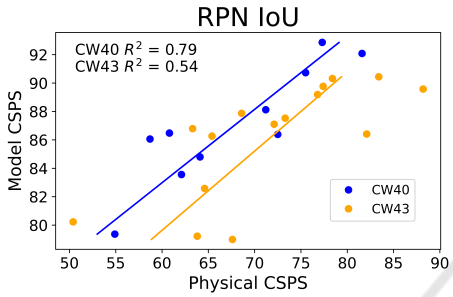

(a)

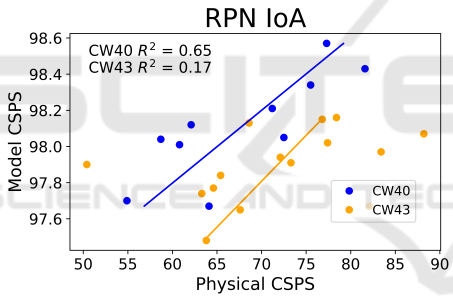

(b)

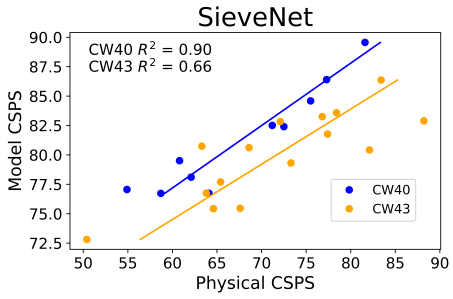

(c)

Figure 4: Correlation plots for the three matching strategies.

multiple predictions, similar that in when using the IoA metric in the RPN. This effect is counteracted when training with more anchor sieves with a consistent increment in diameter as instances are never 100% greater than an associated sieve.

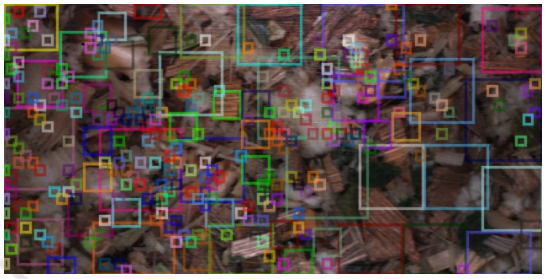

(a)

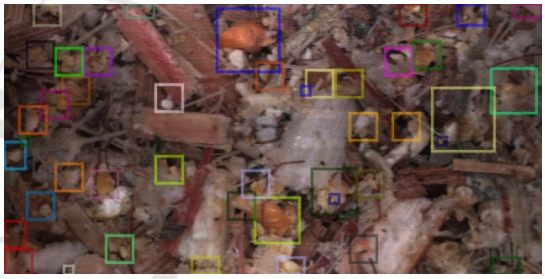

(b)

Figure 5: Two anchors for sieve sizes 1 mm and 4.75 mm. Five anchors for size sizes between 1 mm and 9 mm with 2 mm increments.

In Table 5 the correlation results together with previously presented models are shown for SieveNet with two anchors. The results highlight what was visualised in the image with poor correlation, especially at CW43.

5 CONCLUSION

In this work we present SieveNet, a network able to efficiently monitor WPCS in RGB images captured directly from a forage harvester. We show that localisation of kernel fragments is viable only with an RPN-based architecture reducing the complexity compared to previous approaches based on two-stage recognition networks. Additionally, we introduce an anchor matching algorithm giving the ability to train

networks to classify kernel fragments into predefined sieve sizes. These predictions allow for estimation of CSPS with a strong correlation against physical samples. We believe SieveNet can be extended to other domains where the PSD is also of interest, such as agglomerates or medical imaging, given a definition of appropriate sieved-based anchors.

REFERENCES

Andersson, T., Thurley, M. J., and Marklund, O. (2007). Visibility classification of pellets in piles for sizing without overlapped particle error. In *9th Biennial Conference of the Australian Pattern Recognition Society on Digital Image Computing Techniques and Applications (DICTA 2007)*, pages 508–514.

Drewry, J. L., Luck, B. D., Willett, R. M., Rocha, E. M., and Harmon, J. D. (2019). Predicting kernel processing score of harvested and processed corn silage via image processing techniques. *Computers and Electronics in Agriculture*, 160:144 – 152.

Duan, J., Liu, X., Wu, X., and Mao, C. (2020). Detection and segmentation of iron ore green pellets in images using lightweight u-net deep learning network. volume 32, pages 5775 – 5790.

Fritz, K., Koenig, D., Klauck, U., and Teutsch, M. (2019). Generalization ability of region proposal networks for multispectral person detection. *Automatic Target Recognition XXIX*.

He, K., Zhang, X., Ren, S., and Sun, J. (2016). Deep residual learning for image recognition. In *2016 IEEE Conference on Computer Vision and Pattern Recognition, CVPR 2016, Las Vegas, NV, USA, June 27-30, 2016*, pages 770–778. IEEE Computer Society.

Heinrichs, J. and Coleen, M. J. (2016). Penn state particle separator.

Marsh, B. H. (2013). A comparison of fuel usage and harvest capacity in self-propelled forage harvesters. *International Journal of Agricultural and Biosystems Engineering*, 7(7):649 – 654.

Mertens, D. (2005). Particle size, fragmentation index, and effective fiber: Tools for evaluating the physical attributes of corn silages. *In: Proceedings of the Four-State Dairy Nutrition and Management Conference*.

Rasmussen, C. B., Kirk, K., and Moeslund, T. B. (2021). Anchor tuning in faster r-cnn for measuring corn silage physical characteristics. *Computers and Electronics in Agriculture*, 188:106344.

Rasmussen, C. B. and Moeslund, T. B. (2019). Maize silage kernel fragment estimation using deep learning-based object recognition in non-separated kernel/stover rgb images. *Sensors*, 19:3506.

Ren, S., He, K., Girshick, R., and Sun, J. (2015). Faster r-cnn: Towards real-time object detection with region proposal networks. In *Proceedings of the 28th International Conference on Neural Information Processing Systems - Volume 1*, NIPS'15, page 91–99, Cambridge, MA, USA. MIT Press.

Sharma, K., Gold, M., Zurbruegg, C., Leal-Taixe, L., and Wegner, J. D. (2020). Histonet: Predicting size histograms of object instances. In *Proceedings of the IEEE/CVF Winter Conference on Applications of Computer Vision (WACV)*.

Soloy, A., Turki, I., Fournier, M., Costa, S., Peuziat, B., and Lecoq, N. (2020). A deep learning-based method for quantifying and mapping the grain size on pebble beaches. *Remote Sensing*, 12(21).

Wu, Y., Kirillov, A., Massa, F., Lo, W.-Y., and Girshick, R. (2019). Detectron2. `https://github.com/facebookresearch/detectron2`.

Xu, X., Zhou, F., Liu, B., Fu, D., and Bai, X. (2019). Efficient multiple organ localization in ct image using 3d region proposal network. *IEEE Transactions on Medical Imaging*, 38(8):1885–1898.